

# Tank Leak Detection Using Electrical Resistance Methods

A. Ramirez  
W. Daily  
A. Binley  
D. LaBrecque

This paper was prepared for submittal to the  
*Symposium on the Application of Geophysics to Engineering and Environment*  
*Keystone, CO*  
*April 28-May 1, 1996*

January 1996



Lawrence  
Livermore  
National  
Laboratory

This is a preprint of a paper intended for publication in a journal or proceedings. Since changes may be made before publication, this preprint is made available with the understanding that it will not be cited or reproduced without the permission of the author.

#### DISCLAIMER

This document was prepared as an account of work sponsored by an agency of the United States Government. Neither the United States Government nor the University of California nor any of their employees, makes any warranty, express or implied, or assumes any legal liability or responsibility for the accuracy, completeness, or usefulness of any information, apparatus, product, or process disclosed, or represents that its use would not infringe privately owned rights. Reference herein to any specific commercial product, process, or service by trade name, trademark, manufacturer, or otherwise, does not necessarily constitute or imply its endorsement, recommendation, or favoring by the United States Government or the University of California. The views and opinions of authors expressed herein do not necessarily state or reflect those of the United States Government or the University of California, and shall not be used for advertising or product endorsement purposes.

# **Tank Leak Detection Using Electrical Resistance Methods**

**Abelardo Ramirez<sup>1</sup>, William Daily<sup>1</sup>, Andrew Binley<sup>2</sup>, Douglas LaBrecque<sup>3</sup>**

**1-Lawrence Livermore National Laboratory, Livermore, CA 94550**

**2-Lancaster University, Lancaster, United Kingdom**

**3-University of Arizona, Tucson, Arizona**

## **ABSTRACT**

Two field experiments were performed to evaluate the performance of electrical resistance tomography (ERT) as a leak detection method under metal underground storage tanks (UST). This paper provides a summary of the field experiments performed under a 15 m diameter steel tank mockup located at the Hanford Reservation, Washington. Two different leak events were created. About 3800 liters of saline solution were first released along a portion of the tank's edge and another 1900 liters were later released near the tank's center. The release rate averaged about 26 liters/hour for the leak on the tank's side and about 3.0 liters/hour for the center leak. Two and three dimensional tomographs were calculated using data collected before, during and after each spill. The tomographs show that, as the solution penetrated the soil, readily detectable resistivity decreases appeared where the associated plume was expected. The results indicate that the plume associated with these releases could be reliably detected after approximately 190 liters were released. Results are also shown where the metal tank is used as a large electrode.

## **INTRODUCTION**

Large volumes of hazardous liquids are stored worldwide in surface and underground tanks. Frequently these tanks are found to leak, thereby resulting in not only a loss of stored inventory but, more importantly, contamination to soil and groundwater. The DOE has 332 underground storage tanks at its Hanford, Idaho, Oak Ridge, Fernald, West Valley and Savannah River sites; these store 380,000 cubic meters of high-level waste (HLW) in both liquid and solid forms. The different forms of the waste in the tanks will require a variety of technologies for waste removal and treatment. DOE's single shell tanks present potential environmental hazards because only a single barrier contains the liquids and any breach in the barrier may cause contaminant spillage. One method being considered to retrieve the tank waste is sluicing. This method will require recirculating thousands of gallons of water in the tank. If the sluicing method is used, it is possible to leak HLW into the soil.

There are two methods of detecting leakage from tanks: monitoring the liquid level of waste in the tanks and monitoring the soil under the tanks for leaks. Liquid level sensors can signal a leak but are limited in sensitivity and provide no information about the location or the leak or the distribution of the resulting plume. Outside the tanks detection is more challenging. It is very expensive to emplace chemical sensors under the tanks and the heterogeneous finger-like structure of liquid transport through soils requires that

hundreds of sensors be placed around and underneath a tank to ensure reliable detection of chemical contaminants spills.

The strategy of our approach is to map the resistivity around and below a tank over time. When the spillage of the liquids changes the electrical resistivity in a measurable way, electrical resistivity tomographs can be used to map the resistivity changes caused by spillage. The pixel elements shown in difference resistivity tomographs behave, in some ways, like an array of point sensors deployed below a tank to detect spillage.

This work was designed specifically to address the issues of leaks from the single shell tanks built by the DOE during the cold war for storage of highly radioactive mixed wastes. For this reason a salt water tracer was used in this field demonstration. For testing, an electrical equivalent (saline solution) was used instead of the real contaminant (radioactive nitrate solutions, see Cruse *et al.*, for details) to preserve the environmental quality of the test site. To test the proposed approach in a field demonstration, we would like to produce a tomograph of the soil under a tank and then, while observing changes of subsurface electrical properties, release the contaminant near the tank to simulate a leak.

The test site used for this work is part of the 200 East Area in the Hanford Site, located near Richland, Washington. The near surface sediments at the test site consist primarily of fine to coarse grained sand displaying plane lamination and bedding. The field experiments were performed under a 15.2 m diameter steel tank mockup. Figure 1 shows the layout at the leak detection experiment site. This empty steel tank contained several built-in spill points (two of which are shown). Sixteen boreholes with eight electrodes in each surrounded the tank. The electrodes were located in 10.7 m deep boreholes starting at the ground surface and spaced every 1.52 m. The diametrical distance between boreholes was 20.7 m.

About 3800 liters of saline solution were released along a portion of the tank's edge (side release point in Fig. 1) and another 1900 liters were later released near the tank's center (center release point in Figure 2). The release rate averaged about 26 liters/hour (7 gallons/hour) for the side leak and about 3.2 l/hour (0.85 gals/hour) for the center leak. The fluid was a 0.08 molar sodium chloride solution. This amount of salt increased the conductivity of the solution from about 0.03 to 3.0 S/m. We note that this concentration should be much more dilute than real Hanford tank liquids which are typically fully saturated solutions (about 100 times more concentrated than the brine concentration used for the test). The ERT measurements were made using a pole-pole approach.

ERT surveys were made before, during and after the brine release in each of 8 horizontal planes beneath the tank. Plane 8 is a horizontal cross section at the ground surface 1.5 m above the bottom of the tank (so it contained the tank itself). Plane 7 is 1.5 m lower, a cross section level with the tank bottom. Plane 6 is 1.5 m below the tank bottom and so on to plane 1 which is 10.7 m below the ground surface. This arrangement provided a series of 2D image planes at many levels which, when assembled together, gave an overall 3D view of the plume formed beneath the tank during the release and which could be used to determine the effects of imaging current shunted through the tank bottom.

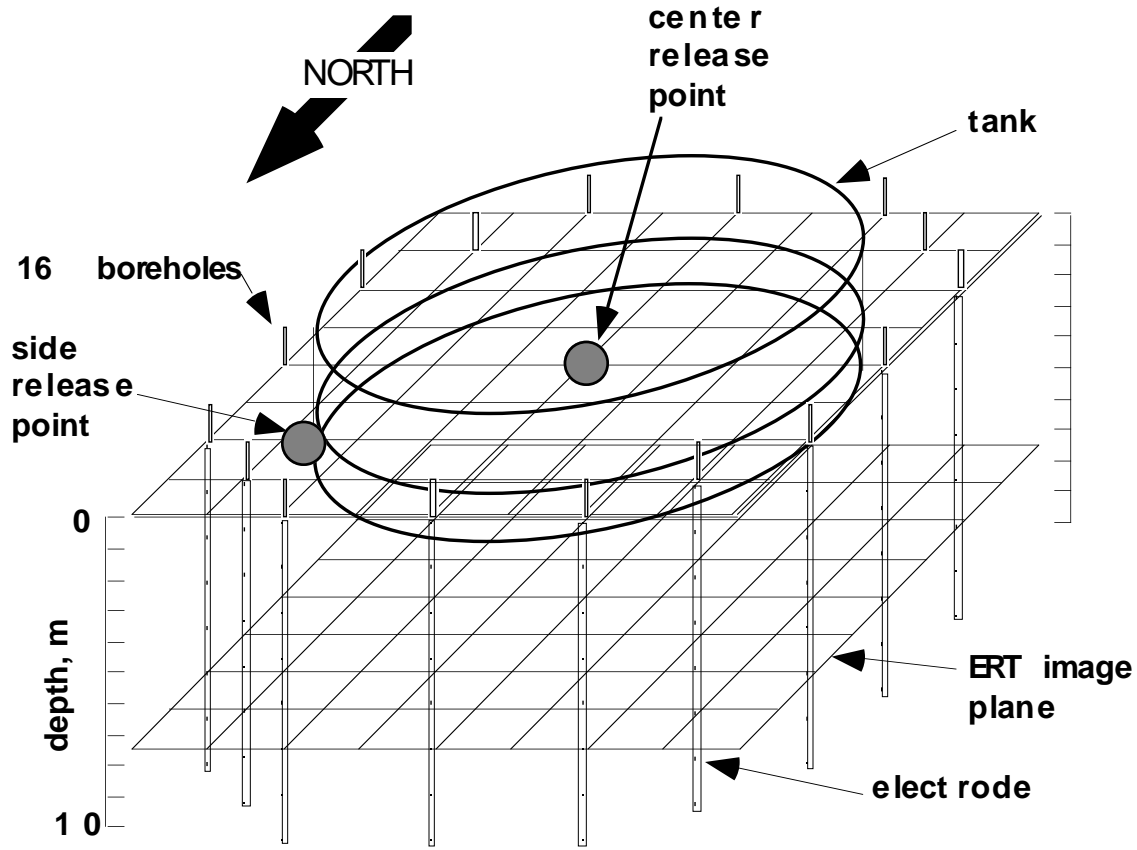


Figure 1. Schematic of experimental set up for leak detection. A 15 m diameter steel tank, the lower 2 meters of which is buried, contains several built-in spill point; results obtained using two of these spill points will be discussed. Sixteen boreholes, with eight electrodes in each, surround the tank.

## DISCUSSION OF RESULTS

To recover the resistivity changes caused by the leak, we compared two sets: 1) a data set measured after the tank release begins and 2) a corresponding data set measured when there is no plume. One may consider performing the analysis by subtracting, pixel by pixel, images without the plume anomaly beneath the tank from those with the plume. However, this approach cannot be used because the two dimensional reconstruction algorithm will not converge using input data for which the boundary conditions are clearly three dimensional--the earth surface and the tank bottom are not accounted for in the forward model of the 2D code. Therefore, the comparison was performed by inverting the quantity

$$\frac{R_a}{R_b} \times R_h \quad (1)$$

where  $R_a$  is the transfer resistance calculated assuming a 3D resistivity model for the case after the release (3D model includes an electrically conductive tank and the plume beneath it),  $R_b$  is the transfer resistance calculated using a 3D model for the case before the release (3D model includes a conductive tank in an homogeneous half space) and  $R_h$

is the calculated transfer resistance for a model of uniform resistivity. The transfer resistance is simply the ratio of voltage to current for an individual 4 electrode measurement. This comparison is a simple perturbation from the uniform resistivity case as described by Daily and Owen (1991).

This paper provides a brief summary of the field results obtained; additional details can be found in Ramirez et al., 1995. Numerical modeling results shown in Ramirez et al. suggest that the data ratio technique described above can yield reasonable results in spite of the fact that neither the ground/air interface nor the tank are included in the 2d model. The algorithm used for this inversions is described by LaBrecque et al. (1995a).

Figure 2 presents two-dimensional (2D) tomographs collected during the course of the side release experiment. The location of the release point is indicated on the figure. The images show which areas of the soil changed in response to the brine spill. Each column of images shows the changes detected for a given time at various depths; the depth of images on each column increases from top (0 m. depth to bottom (10.7 m depth). Time and leaked volume increase from left to right on the figure. The images for July 26 at depths of 1.5 and 3 m (the top two available images of the first column in Figure 2; the top two planes were not collected at this time) show clearly detectable electrical conductivity increases directly below the release point close to the "path for vertical migration". This behavior suggests that the brine is moving almost straight down as may be expected in reasonably homogeneous sandy soil present at the experimental site. Note that the changes observed increase in magnitude as time and spilled volume increase. Also, note that the bottom of the changing region deepens as time increases.

Electrical noise measurements were also made during the tests by comparing each measurement with its reciprocal. These measurements were then used to calculate reconstructions which showed the magnitude of changes in the images expected from measurement error. The worst case of these "noise" images showed the resistivity ratio to deviate from 1.0 (i.e., perfect result when no changes occur) by  $\pm 0.005$ . This analysis shows that resistivity changes shown in Figure 2 are much bigger (resistivity ratios are much smaller) than those changes which could be expected due to measurement error. The analysis assumes that the differences between the normal and reciprocal measurements provide good estimates of the measurement errors.

The images in Figure 2 are consistent with the behavior expected for infiltration of water released into a fairly homogeneous unsaturated sand. There is a clear decrease in resistivity of the volume directly below the release point from which the plume appears to drain downward by gravity and spreads laterally by capillary suction and as it encounters soil heterogeneity. The approximate leak location can be estimated as the point directly above the region of maximum change in the top few planes. The lateral and vertical extent of the plume as a function of time can also be roughly estimated from the images. The aggregate of these results is consistent with intuition. We maintain that, in the absence of independent corroborating data, this fact supports the hypothesis that the tomographs are credible representations of the released brine.

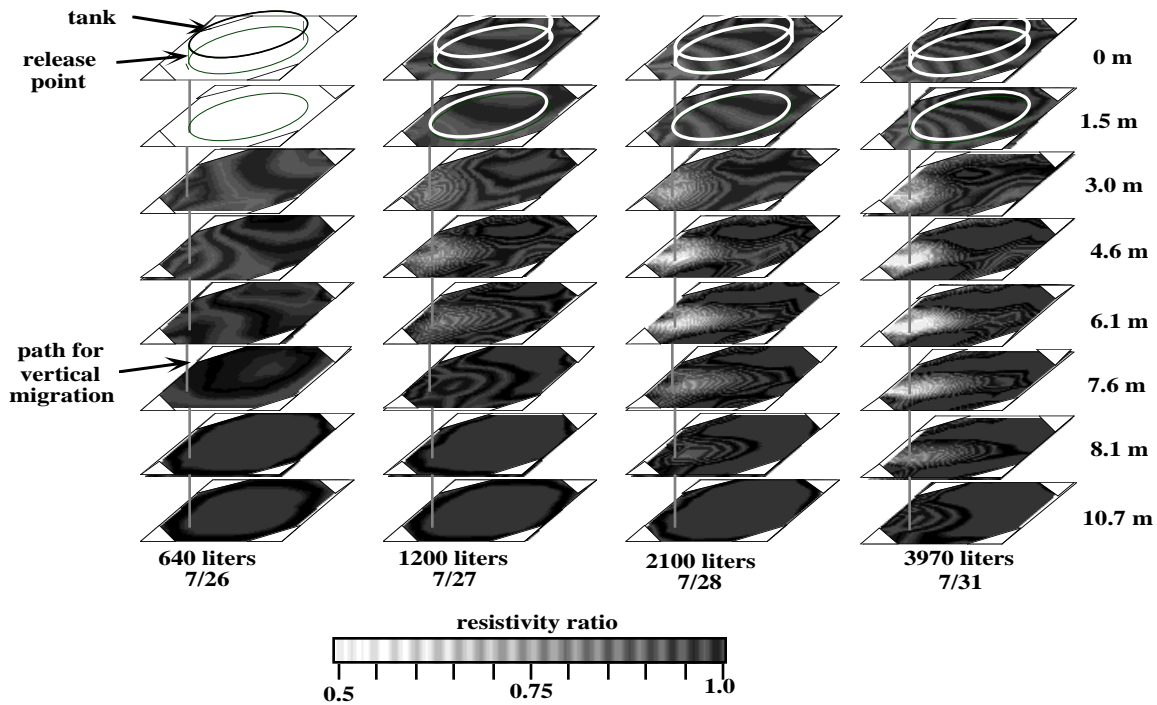


Figure 2. A series of two-dimensional ERT tomographs which show how the electrical conductivity of the soil increased during the side release experiment. Black on the gray scale indicates which portions of the images remain unchanged. Shades of gray to the left of black indicate which portions of the image show electrical conductivity increases associated with the leak.

Figure 3 shows three dimensional ERT tomographs generated from data collected during the side leak. In this case, the data are used to calculate the resistivity changes within a block underneath the tank (instead of as a series of two dimensional slices shown in Figure 2) using only data from electrodes located at 1.5 m, 6.1 and 10.7 m depth.

The three dimensional inversion explicitly accounts for the metal structure. This is in contrast to the approach used for the 2d inversions. Thus, one may expect that the 3D results should be more accurate than the 2D results. However, the calculation times for the 3D inversions are about 40 times longer than for the 2D inversions covering the same volume. A description of the 3D inversion algorithm is described by LaBrecque et al., 1995b.

It is necessary to calculate the electric field near the metal-soil boundary during forward modeling by the 3D code. The resistivity contrast between the soil and the metal can be as high as  $10^9$ ; for comparison, normal geologic systems have contrasts which are about  $10^2$ . Around the steel tank is a layer of metal oxide which also affects the resistivity contrast. The transition from the metal and oxide layers to the soil occurs over a very short distance (roughly 1 cm). The large resistivity contrast across these layers requires that accurate forward solvers be used to obtain accurate calculation of the electric field. However, the inverse problem is regularized, meaning that inversion finds the smoothest

resistivity structure which fits the data to some tolerance. The algorithm will tend to find resistivity models where there is minimal contrast between an element and its neighbors. It is necessary to modify the inversion algorithm because of the tank and soil. Otherwise, the resistivity associated with the tank will be "smeared" to the surrounding elements representing the soil and yield erroneous values. The algorithm used for this inversion was modified to allow for a non-smooth solution at the tank boundary.

The 3D reconstruction shown in Figure 3, is 21.3 m wide, 21.3 m. long and 10.7 m. tall and is the reconstructed volume bounded by the electrode arrays in the sixteen holes around the tank. Those parts of the reconstruction with resistivity differences between 0 and -150 ohm-m are shown as transparent so that the interior of the block can be observed. Note that the 2D reconstructions in Figure 2 and 3D images in Figure 3 show the same approximate position, shape and size of the anomaly over time. The 3D images may provide a better view of the changes caused by the leak because: a) the flow regime is truly three-dimensional, so there is no need to assume that the resistivity extends to infinity in the third dimension, b) there is no need for interpolation between adjacent 2D slices, and, c) the effect of the metallic barrier is explicitly accounted for in the 3D images but not in the 2D images. However, the 3D images takes much longer to calculate (5 days per block) than the 2D images (20 minutes per plane).

Numerical modeling results suggest that the position of the anomaly has a significant effect on the results observed. Changes below the tank's center are observed with much less sensitivity than changes near the side of the tank. The modeling results suggest that anomalies closer to the electrodes are observed with greater sensitivity. If the tank itself is used as one large electrode, it may offer increased sensitivity and resolution because it is located closer to the leak point than any other electrode.

Figure 3 illustrates the effects of using the tank as an electrode. The figure compares two resistivity difference tomographs. The one on the left shows the results when only hole to hole data is used. The right image in Figure 3 shows the results when the tank is used in combination with the boreholes electrodes, i.e., hole to hole measurements and hole to tank measurements were used in combination. The difference image on the left of the figure is more elongated than the image on the right, which is more spherical. We do not have independent data that can be used to determine which of the two results is closer to the true structure. However, we speculate that the image on the right may more closely represent the true structure because the spherical shape is closer to what may be expected for a reasonably homogeneous sandy soil such as what exists at the experimental site.

The 3d algorithm can also be used to model the effects of metal cased boreholes. Some of the metal tanks at the Hanford site are surrounded by metal cased vertical boreholes (Cruse *et al.*, 1995). One approach considered in our work is to use these metal cased boreholes as long electrodes for ERT leak detection. The test site described in Section 2.2 and Figure 2 was modified to create an electrical analog to a tank surrounded by 4 metal cased boreholes and 4 normal ERT electrode boreholes. To approximate a metal cased borehole, the eight electrodes in an ERT borehole were shorted together, creating a piecewise continuous electrode between the top and bottom electrode. Every other ERT hole was used as a "metal casing analog". The data were inverted using the 3D resistivity algorithm and the "metal casing analogs" were modeled as vertical columns of highly conducting elements which extended from the ground surface to 10.7 m depth.

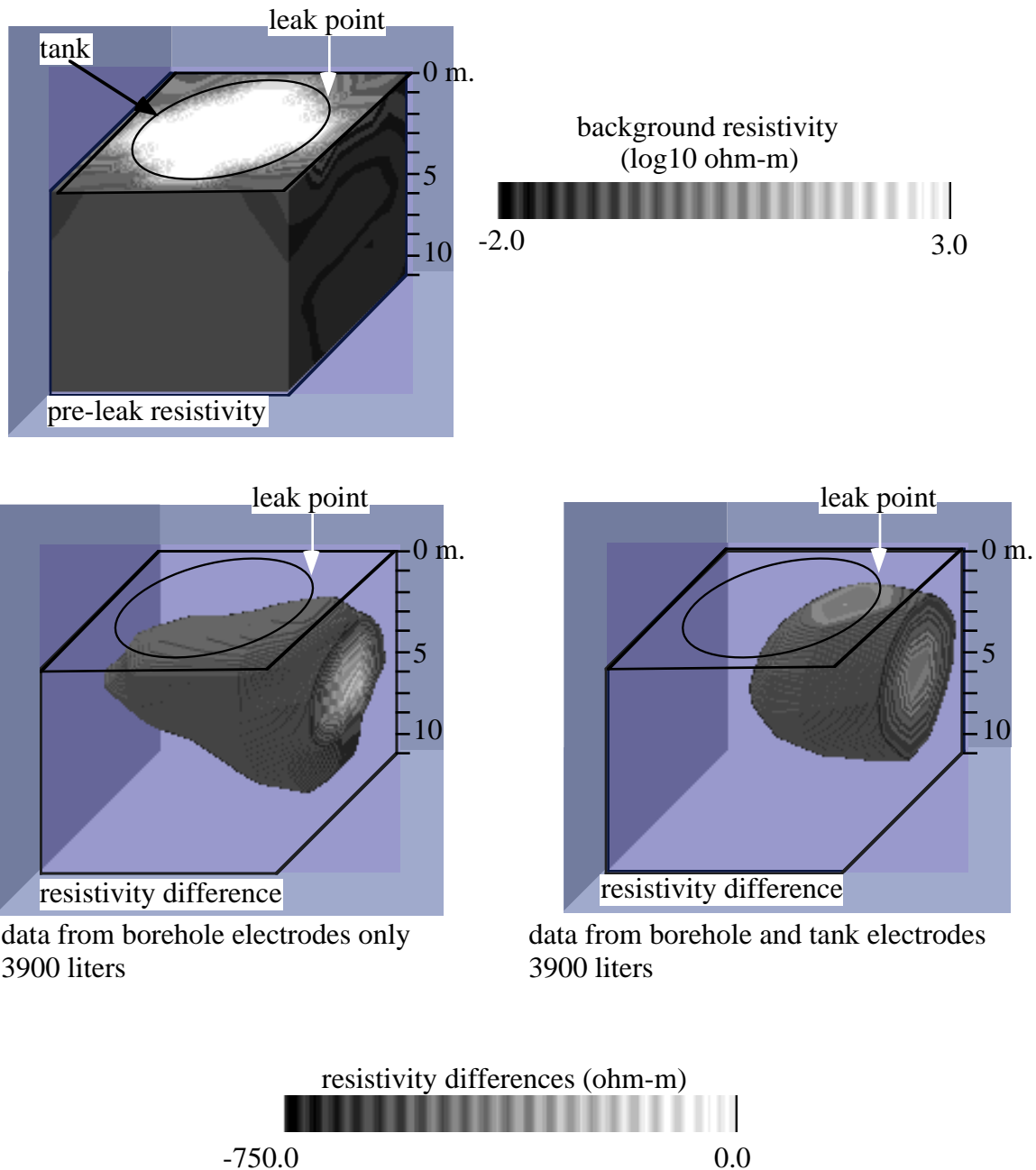


Figure 3 shows how the resistivity tomographs change when the tank is used as an electrode in combination with electrodes in the boreholes. The bottom two images show resistivity differences on the last day of the release; these images are transparent where the resistivity differences observed were less than 150 ohm-m. The data for the top left and bottom left images was collected using only the electrodes in the boreholes. The data for the right image was collected using the tank as an electrode as well as the borehole electrodes.

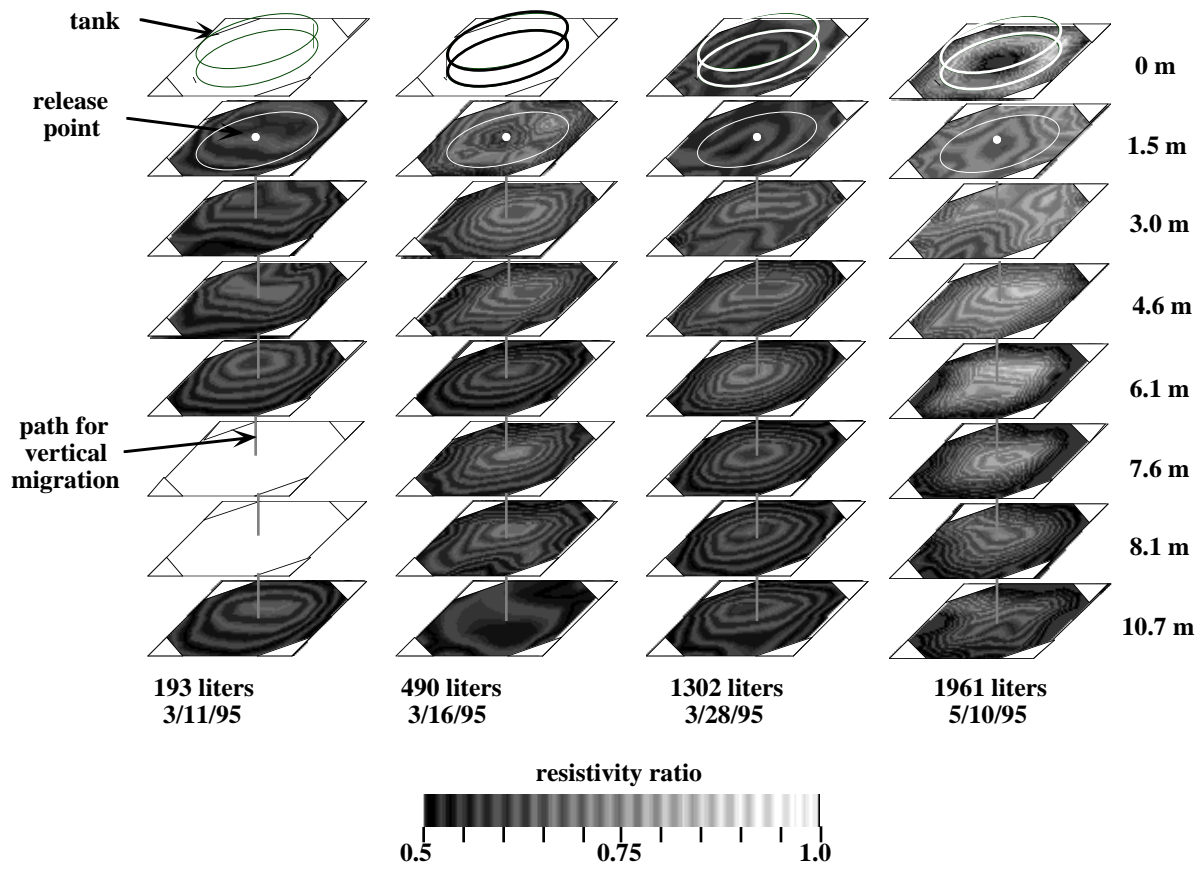


Figure 4 shows a series of two-dimensional ERT tomographs which show how the electrical resistivity of the soil decreased during the center release experiment. The range of values represented by the grey level used is identical to that used to depict the side release results in Figure 2. A vertical dotted line shows the trajectory the brine would follow if it moved straight down.

Ramirez et al., 1995, show resistivity differences obtained when four "metal casing analogs" along with four normal electrode boreholes (with eight electrodes in each borehole) were used during the center release. These results suggest that metal cased boreholes used as long electrodes, in combination with normal ERT electrodes, can be used to calculate reasonable images of resistivity changes caused by the leak.

Figure 4 presents two-dimensional (2D) tomographs collected during the course of the center release experiment (spill point location shown in Figure 2). Time and leaked volume increase from left to right on the figure. The images for March 11 show clearly detectable electrical conductivity increases below the release point and extending to the South and East. The changes observed increase in magnitude as time and spilled volume increase just as was observed during the side release. Also, note that the bottom of the changing region extends deeper as time increases. This behavior suggests that the brine is moving mainly down with some movement to the SE. The movement to the SE may be explained by the slight SE dip of the sand layers at the site.

The results obtained early during the middle release show that reliable changes associated with the leak were detected after 190 liters (50 gals.) had been released. These results are shown in Figure 4, left hand column of images. Note that data was not collected when

the released volume was smaller than 190 liters. It is possible that volumes smaller than 190 liters are detectable.

We believe that some of the images in Figure 4 are distorted; anomaly distortions can be expected when the horizontal image plane is in close proximity to the tank. For example, note the images at 1.5 and 3.0 m depth on 5/10/95. These images suggest that the whole region between the boreholes has decreased in resistivity; we believe that the width of the anomaly has been greatly exaggerated in these cases due to the minimal resolution of targets located just below the tank near the image center.

Electrical noise measurements were also made during the center release test. The results from these tests showed the same noise effect on the image as observed during the side release, i.e., ratios larger than 0.995 could be caused by noise. The resistivity ratios shown in Figure 4 are much smaller (i.e., represent larger changes) than those changes caused by measurement error. Note that resistivity ratios of approximately 0.94 were observed on 3/11 after 193 liters (about 50 gallons) had been spilled. These results imply that volumes of brine larger than 190 liters released from the center of the tank should be readily detectable, when site conditions are similar to those at the test site.

#### SUMMARY AND CONCLUSIONS:

The results from two field experiments have been presented to illustrate the performance of ERT to detect leaks beneath a metal tank and to map the resulting plumes. The approach described here relies on detection and mapping of the changes in electrical resistivity associated with a leak. Many liquids released from tanks can create changes in a soil's electrical properties that are readily measured. Electrical resistance tomography is used as an inversion technique to map the soil's electrical resistivity in two and three dimensional space.

The 2D field results from both the side release and center release tests are consistent with the behavior expected for infiltration of water released into a fairly homogeneous unsaturated sand. There is a clear decrease in resistivity of the volume directly below the release point from which the plume appears to drain downward by gravity. For the side release, the approximate leak location can be found directly above the region of maximum change in the top few planes. The lateral and vertical extent of the plume as a function of time can also be roughly estimated from the images. The center release results are consistent with the side release; the primary difference is that the center leak anomalies are, in general, wider than those for the side leak due to decreased resolution near the images' center. These results suggest that ERT detected the brine released from both leak locations and could follow its downward propagation. The location, magnitude and time behavior of the anomaly observed during the brine spill is consistent with the hypothesis that the anomaly was caused by the leakage and not by unrelated phenomena such as electrical noise.

The 3D results from the side release show reasonable agreement with the 2D results. One advantage of 3D inversions is that large metal structures such as the tank itself and metal cased boreholes can be modeled, and thus used as electrodes. The field results suggest that metal cased boreholes may be used as electrodes in combination with point electrodes located in other boreholes and that this approach yields reasonable results.

By the time the first measurements during either spill had been made, the resistivity had changed approximately 5%, it may be possible that smaller changes are detectable. Noise analysis results suggest that it may be possible to see changes as small as 2%.

## Acknowledgments

The work of many people was needed to ensure the success of this project. D. Iwatate and J. Propson under W. Miller, Westinghouse Hanford Co., TWRS/ Engineering. Specialties Group, coordinated site activities, helped plan the tests, and served as liaison to tank operation activities. ICF Kaiser Hanford provided construction and site maintenance support. J. J. Carbino (LLNL) coordinated the installation and construction of all the ERT hardware installed in the boreholes and assisted in data collection.

This work was performed under the Environmental Technologies Program at LLNL. It was funded by the Characterization, Monitoring and Sensors Tech. Program, Office of Technology Development, U.S. Department of Energy (DOE). The DOE - Richland Operations Office provided funds to prepare and maintain the experimental test site at Hanford. Work performed under the auspices of the U.S. Department of Energy by Lawrence Livermore National Laboratory under Contract W-7405-ENG-48.

## REFERENCES

Cruse, J., D. Iwatate, K. Tollefson, R. Treat, T. Trenkler, and R. Lewis, 1995, Functions and Requirements for Hanford Single-Shell Tank Leakage Detection and Monitoring, WHC-SD-WM-FRD-021, Westinghouse Hanford Co, Richland, WA.

Daily, W. and E. Owen, Cross Borehole Resistivity Tomography, 1991, *Geophysics*, 56, 1228-1235.

LaBrecque, D. J., William Daily, Earle Owen and Abelardo Ramirez, 1995a, Noise and OCCAM's Inversion of Resistivity Tomography Data, *Geophysics*, in press.

LaBrecque, D. J., G. Morelli, W. Daily, A. Ramirez, and P. Lundegard, 1995b, OCCAM's Inversion of 3D ERT Data, Proc. of the International Symposium on Three Dimensional Electromagnetics, Richfield, Connecticut, pp. 471-482.

Ramirez, A., W. Daily, A. Binley, D. LaBrecque, and D. Roelant, 1995, Detection of Leaks from Underground Storage Tanks Using Electrical Resistance Tomography, Lawrence Livermore Nat. Laboratory, UCRL-JC-122180, Livermore, CA.